Molecular magnets based on chain polymer complexes of copper(II) bis(hexafluoroacetylacetonate) with isoxazolyl-substituted nitronyl nitroxides

S. V. Fokin, S. E. Tolstikov, E. V. Tretyakov, G. V. Romanenko, A. S. Bogomyakov, S. L. Veber, R. Z. Sagdeev, and V. I. Ovcharenko★

International Tomography Center, Siberian Branch of the Russian Academy of Sciences, 3a ul. Institutskaya, 630090 Novosibirsk, Russian Federation. Fax: +7 (383) 333 1399. E-mail: Victor.Ovcharenko@tomo.nsc.ru

First isoxazolyl-substituted nitronyl nitroxides (L and L^{Me_2}) were synthesized and characterized. Their reactions with $Cu(hfac)_2$ and $Mn(hfac)_2$ (hfac is hexafluoroacetylacetonate) afford the heterospin complexes $[Cu(hfac)_2L]_n$, $[Cu_2(hfac)_4L]_n$, $[Cu_2(hfac)_4L^{Me_2}]_n$, $[Cu(hfac)_2L^{Me_2}]_n$, $[Cu(hfac)_2L^{Me_2}{}_2]$, $[Cu(hfac)_2L^{Me_2}(MeCN)]$, $[Mn(hfac)_2]_3L_4$, and $[Mn(hfac)_2L^{Me_2}]_2$. In the ligand L, the N atom of the isoxazole ring (N_{Iz}) has weak electron-donating properties. For example, the paramagnetic ligand in the chain polymer complex $[Cu(hfac)_2L]_n$ acts as a bidentate bridging ligand coordinated through both O atoms of the nitronyl nitroxide group (O_{N-O}); the N_{Iz} and O_{Iz} atoms are not involved in the coordination. The introduction of Me groups into the isoxazole substituent results in an increase in the electron density on the N_{Iz} atom and enables the synthesis of the chain polymer complex $[Cu(hfac)_2L^{Me_2}]_n$, in which the bidentate bridging ligand L^{Me_2} is coordinated through the O_{N-O} and N_{Iz} atoms. In the mononuclear complexes $[Cu(hfac)_2L^{Me_2}{}_2]$ and $[Cu(hfac)_2L^{Me_2}(MeCN)]$, the paramagnetic ligand is coordinated only through the N_{Iz} atom. The solid heterospin Mn complexes $[Mn(hfac)_2]_3L_4$ and $[Mn(hfac)_2L^{Me_2}]_2$ have a molecular structure. In these complexes, strong antiferromagnetic intracluster exchange interactions arise. The residual magnetic moments of the exchange clusters in the complex $[Mn(hfac)_2]_3L_4$ are ferromagnetically coupled, resulting in the increase in the effective magnetic moment (μ_{eff}) of the complex with decreasing temperature in the range of 300—30 K. The thermomagnetic study of the complexes $[Cu(hfac)_2L]_n$, $[Cu_2(hfac)_4L]_n$, and $[Cu_2(hfac)_4L^{Me_2}]_n$ in the range of 2—300 K revealed the ferromagnetic ordering at temperatures below 5 K. The ESR study of the solid complex $[Cu(hfac)_2L^{Me_2}]_n$ showed that the decrease in its μ_{eff} in the temperature range of 30—300 K is associated with the direct exchange interaction between the unpaired electrons of the nitronyl nitroxides of adjacent chains, whereas at temperatures below 30 K, only Cu^{2+} ions contribute to the magnetic susceptibility of the complex.

Key words: copper(II) complexes, manganese(II) complexes, coordination compounds, magnets, nitroxides, hexafluoroacetylacetonates, X-ray diffraction analysis, magnetic measurements.

Magneto-structural relationships inherent in "breathing" crystals based on heterospin mixed-ligand coordination compounds $[Cu(hfac)_2L^{Pz(R)}]_n$ (hfac is hexafluoroacetylacetonate, $L^{Pz(R)}$ is spin-labeled alkyl-substituted pyrazole) are extensively studied nowadays.

Solid phases of these compounds are formed by polymer chains composed of alternating bis-chelate fragments and spin-labeled ligands. The characteristic feature of the crystals of $[Cu(hfac)_2L^{Pz(R)}]_n$ is that they can undergo thermally induced structural rearrangements in the solid state accompanied by magnetic anomalies, which are similar in character to the temperature dependences of the effective magnetic moment (μ_{eff}) to the spin crossover phenomenon.[1—28]

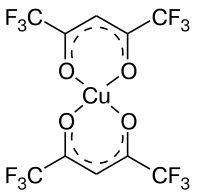

$Cu(hfac)_2$

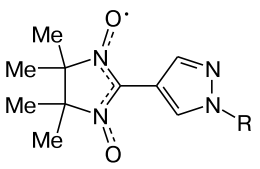

$L^{Pz(R)}$

R = H, Me, Et, Pr, Pr^i, Bu, CD_3, C_2D_5

The investigation of the magnetic properties of the compounds $[Cu(hfac)_2L^{Pz(R)}]_n$ showed that the variation of the alkyl substituent R in the ligand $L^{Pz(R)}$ has a sub-

Published in Russian in *Izvestiya Akademii Nauk. Seriya Khimicheskaya,* No. 12, pp. 2423—2436, December, 2011.

stantial effect on the character of the dependence $\mu_{eff}(T)$ and the spin-transition temperature. This stimulated us to synthesize and investigate complexes with spin-labeled isoxazolyl-substituted paramagnetic ligands L and L^{Me_2} containing no such substituents in the aromatic ring.

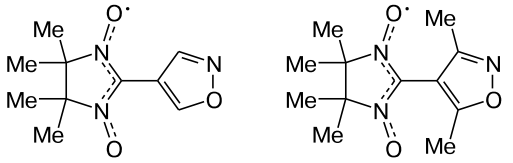

L L^{Me_2}

Results and Discussion

The ligand L was synthesized according to the classical scheme involving the transformation of iodoisoxazole **1a** into isoxazole-4-carbaldehyde **2a** and the condensation of the latter with 2,3-bis(hydroxyamino)-2,3-dimethylbutane (**3**) followed by the oxidation of product **4a** to give the target nitronyl nitroxide L (Scheme 1). A similar procedure was used for the synthesis of L^{Me_2}.

Scheme 1

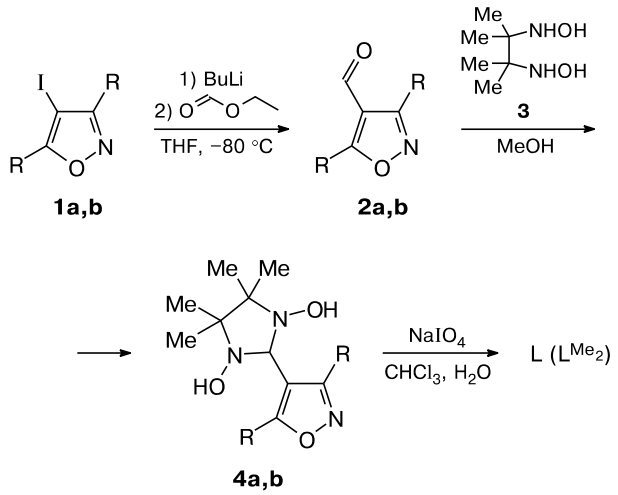

R = H (**a**), Me (**b**)

The single-crystal X-ray diffraction study showed that the isoxazole rings in the molecules L and L^{Me_2} (Fig. 1) are virtually planar, with the deviations of the atoms from the mean plane passing through all atoms of the rings within 0.01 Å. The imidazoline rings adopt a typical *gauche* conformation, with the C atoms being located on the opposite sides of the plane passing through the atoms of the ONCNO group. The deviations of these C atoms are within ±0.15 and ±0.28 Å in the ligands L and L^{Me_2}, respectively. The angle between the planes of the isoxazole ring and the ONCNO fragment is 9.5 and 45.2° in L and L^{Me_2}, respectively. The molecule L has a twofold symmetry axis C_2 passing through the C atoms that link the heterocycles. Hence, the N and O atoms of the isoxazole ring of the ligand L were specified as (0.5N + 0.5O). In L^{Me_2}, in spite of the asymmetry of the molecule, the positions of the N and O atoms in the isoxazole ring were not reliably determined and, consequently both atoms were specified as (0.5N + 0.5O). The N—O bond lengths in the ONCNO fragments are 1.276(2) and 1.279(2) Å for L and L^{Me_2}, respectively, which is typical of nitronyl nitroxide radicals.[29]

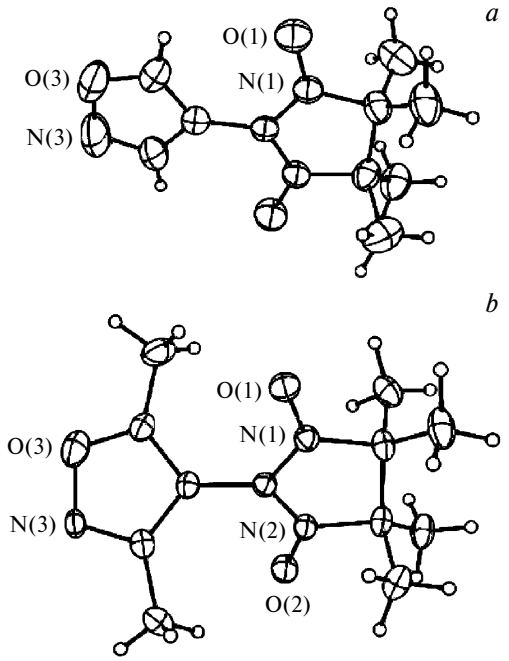

Fig. 1. Molecular structures of L (*a*) and L^{Me_2} (*b*). The displacement ellipsoids are drawn at the 35% probability level.

In the solid ligand L, the O...O distances between the O atoms of the N—O groups are 3.60 Å. This distance is larger than the corresponding alternating distances in the crystals of L^{Me_2} (3.28 and 3.48 Å). Apparently, the shorter distances between the paramagnetic centers (PMC) in solid L^{Me_2} are responsible for stronger antiferromagnetic exchange interactions between the unpaired electrons of PMC compared to the corresponding interactions in the ligand L. We did not specially investigate the cause of the stronger exchange in solid L^{Me_2}. Let us only note that the high-temperature asymptotics of μ_{eff} of the nitronyl nitroxides (Fig. 2) are close to 1.73 μ_B, which corresponds to the electron-only momentum for a particle with $S = 1/2$ and $g = 2$.

It was found that the reaction of $Cu(hfac)_2$ with L can afford two compounds, whose compositions correspond to the formulas $Cu(hfac)_2L$ and $Cu_2(hfac)_4L$, the latter being obtained only when the reaction was performed in hexane using the reagents in the ratio $Cu(hfac)_2 : L = 2 : 1$.

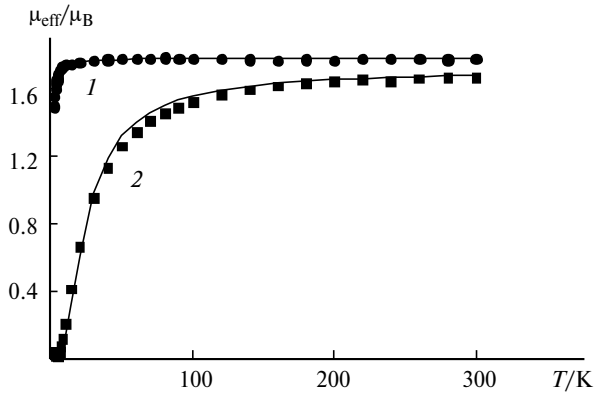

Fig. 2. Temperature dependences of the effective magnetic moment (μ_{eff}) for L (*1*) and L^{Me_2} (*2*). Solid lines represent the optimal theoretical curves with the parameters $g = 2.056$, $J/k = -0.99$ K and $g = 2.0$, $J/k = -33.9$ K for L and L^{Me_2}, respectively.

In other solvents (CH_2Cl_2, CH_2Cl_2—hexane, toluene), the reaction with the use of the reagents in the same ratio afforded a mixture of $Cu(hfac)_2L$ and excess $Cu(hfac)_2$ as the solid products. In the case of the equimolar ratio of the reagents, the complex with the ratio $Cu(hfac)_2 : L = 1 : 1$ crystallized out from all solvents.

The solid phases of the heterospin complexes under consideration are composed of the polymer chains $[Cu(hfac)_2L]_n$ and $[Cu_2(hfac)_4L]_n$ (Fig. 3). The nitronyl nitroxide radical in both $[Cu(hfac)_2L]_n$ and $[Cu_2(hfac)_4L]_n$ serves as the O,O´-bridging ligand, whose N—O groups (see Fig. 3, the O(02) and O(01) atoms) are coordinated to the alternating $\{Cu(hfac)_2\}$ fragments. The coordination environment of the Cu atom can be described as an elongated octahedron with the equatorial $Cu—O_{hfac}$ distances not exceeding 1.95 Å and the axial $Cu—O_{N—O}$ distances being 2.422(2) and 2.417(2) Å in $[Cu(hfac)_2L]_n$ and 2.412(5) and 2.468(5) Å in $[Cu_2(hfac)_4L]_n$. The angles at the coordinatively bound $O_{N—O}$ atoms are substantially different. In $[Cu(hfac)_2L]_n$, these angles are 128.5(1) and 138.9(2)°; in $[Cu_2(hfac)_4L]_n$, 151.0(5) and 140.3(4)°. The terminal $Cu(hfac)_2$ fragments in $[Cu_2(hfac)_4L]_n$ are linked to the polymer chain through the N (N(3)) atom of the isoxazole ring (N_{Iz}) (see Fig. 3, *b*), which occupies the apical position in the square-pyramidal coordination en-

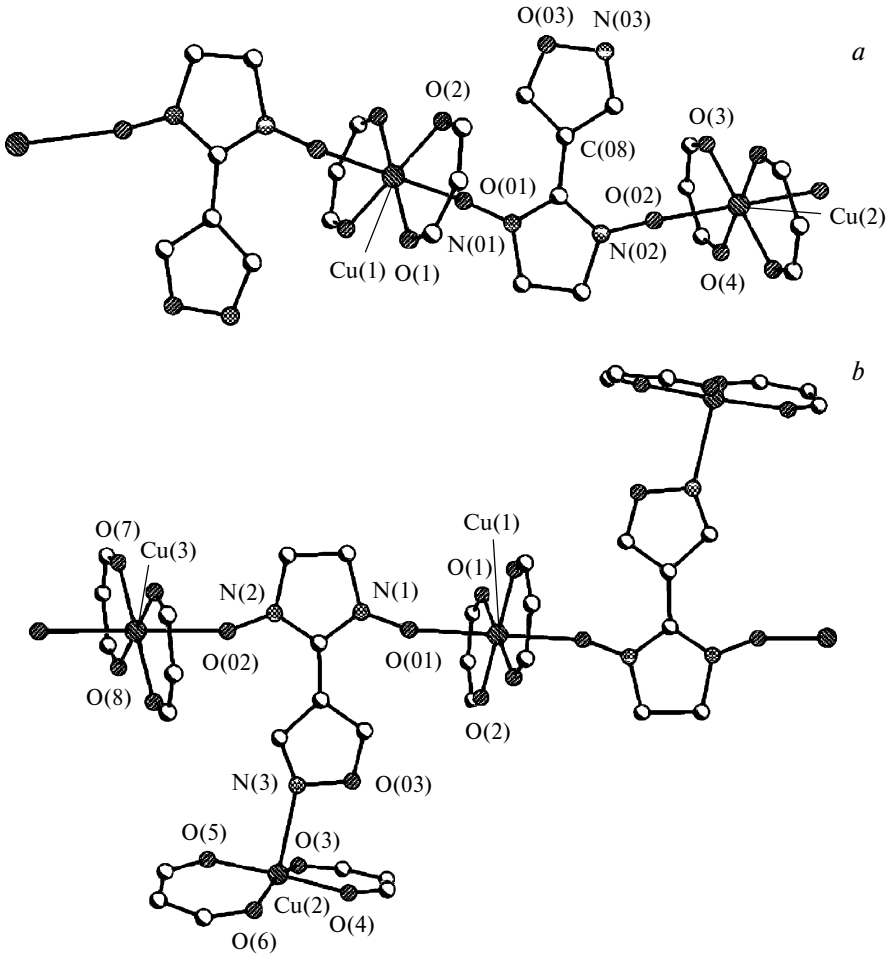

Fig. 3. Fragments of the polymer chains in the complexes $[Cu(hfac)_2L]_n$ (*a*) and $[Cu_2(hfac)_4L]_n$ (*b*).

Table 1. Selected bond lengths (d) and bond angles in the ligands L and L^{Me_2} and their complexes

Compound	d/Å					M—O_{N-O}—N Angle /deg
	M—O_{N-O}	M—N_{Iz}	N—O_{N-O}	N_{Iz}—O_{Iz}	O_{N-O}...O_{N-O}	
L	—	—	1.2767(17)	1.422(3)	3.598	—
L^{Me_2}	—	—	1.279(2), 1.279(2)	1.422(2)	3.282, 3.479	—
$[Cu(hfac)_2L]_n$	2.422(2), 2.417(2)	—	1.287(2), 1.310(3)	1.434(5)	—	128.5(1), 138.9(2)
$[Cu_2(hfac)_4L]_n$	2.412(5), 2.468(5)	2.369(6)	1.285(7), 1.268(7)	1.411(8)	—	151.0(5), 140.3(4)
$[Cu(hfac)_2L^{Me_2}]$	—	2.458(3)	1.276(3), 1.279(3)	1.412(3)	3.483, 3.340	—
$[Cu(hfac)_2L^{Me_2}(MeCN)]$	—	2.357(3)	1.286(3), 1.280(3)	1.417(2)	3.341, 3.452	—
$[Mn(hfac)_2L^{Me_2}]_2$	2.137(2), 2.118(1)	2.348(2), 2.319(2)	1.299(2), 1.276(3), 1.299(2), 1.276(2)	1.411(2), 1.416(2)	3.321, 3.908	131.3(1), 129.7(1)
$[Mn_3(hfac)_6L_4]$	2.134(3), 2.172(3), 2.198(3)	—	1.301(4), 1.274(5), 1.312(4), 1.285(5)	1.427(6), 1.422(5)	2.693	128.5(3), 126.3(3), 128.2(3)

vironment around the metal atom (d(Cu—N) = 2.369(6) Å). As a result, the paramagnetic ligand in the structure of $[Cu_2(hfac)_4L]_n$ is coordinated in a tridentate-bridging mode. The N—O bond lengths in $[Cu(hfac)_2L]_n$ and $[Cu_2(hfac)_4L]_n$ are in the range from 1.268(7) to 1.310(3) Å typical of nitroxides (Tables 1 and 2).

The magnetic properties of the complex $[Cu(hfac)_2L]_n$ deserve special attention. The dependence $\mu_{eff}(T)$ for this compound is shown in Fig. 4, *a*. It can be seen that the magnetic moment μ_{eff} changes only slightly in the temperature range between 100 and 300 K. The high-temperature value of μ_{eff} (2.66 μ_B at 300 K) agrees well with the theoretical spin-only value (2.45 μ_B) for two noninteracting PMC with spins $S = 1/2$ and $g = 2$. At temperatures below 100 K, the value of μ_{eff} sharply increases. This character of the dependence $\mu_{eff}(T)$ is indicative of ferromagnetic exchange interactions between the unpaired electrons of PMC, which is consistent with the X-ray diffraction data on the axial coordination of the nitroxide fragments to the Cu^{2+} ions with distances larger than 2.4 Å. According to the results of theoretical studies,[30,31] this geometry of the coordination unit provides the orthogonal arrangement of the spins in the exchange cluster {ONCNO—Cu^{2+}}. At low temperatures, the magnetization (σ) of $[Cu(hfac)_2L]_n$ nonlinearly depends on the external magnetic field (H) (see Fig. 4, *b*). The spontaneous magnetization (σ_0) assessed from the analysis of the dependence

$$\sigma = \sigma_0 + \chi H,$$

where χ is the magnetic susceptibility of the sample and H is the strength of the applied magnetic field (10230 G cm^3 mol^{-1} at 2 K). This result is close to the theoretical value (11170 G cm^3 mol^{-1}) for two paramagnetic centers with spins $S = 1/2$. The Curie temperature (T_C) for $[Cu(hfac)_2L]_n$ can be estimated as $T_C \leq 3$ K.

The dependence $\mu_{eff}(T)$ for $[Cu_2(hfac)_4L]_n$ is similar to that for $[Cu(hfac)_2L]_n$. At temperatures ranging from

Table 2. Temperature dependence of the selected bond lengths and bond angles in the complexes $[Cu_2(hfac)_4L^{Me_2}]_n$ and $[Cu(hfac)_2L^{Me_2}]_n$

Parameter	$[Cu_2(hfac)_4L^{Me_2}]_n$		$[Cu(hfac)_2L^{Me_2}]_n$			
	47 K	240 K	55 K	100 K	150 K	240 K
Bond/Å						
Cu—O_{N-O}	2.473(3), 2.417(3)	2.522(2), 2.487(2)	2.4159(14)	2.4243(14)	2.4443(16)	2.474(2)
Cu—N_{Iz}	2.256(4)	2.271(3)	2.4711(15)	2.4796(15)	2.4876(18)	2.503(2)
N—O_{N-O}	1.282(4), 1.288(4)	1.287(3), 1.275(3)	1.280(2), 1.273(2)	1.281(2), 1.274(2)	1.275(2), 1.277(2)	1.273(3), 1.271(3)
N_{Iz}—O_{Iz}	1.406(4)	1.404(3)	1.416(2)	1.414(2)	1.414(2)	1.411(3)
O_{N-O}...O_{N-O}	—	—	3.159	3.167	3.176	3.190
Angle/deg						
Cu—O_{N-O}—N	146.5(3), 148.7(2)	146.9(2), 146.5(2)	153.88(11)	153.81(11)	153.56(12)	153.47(15)

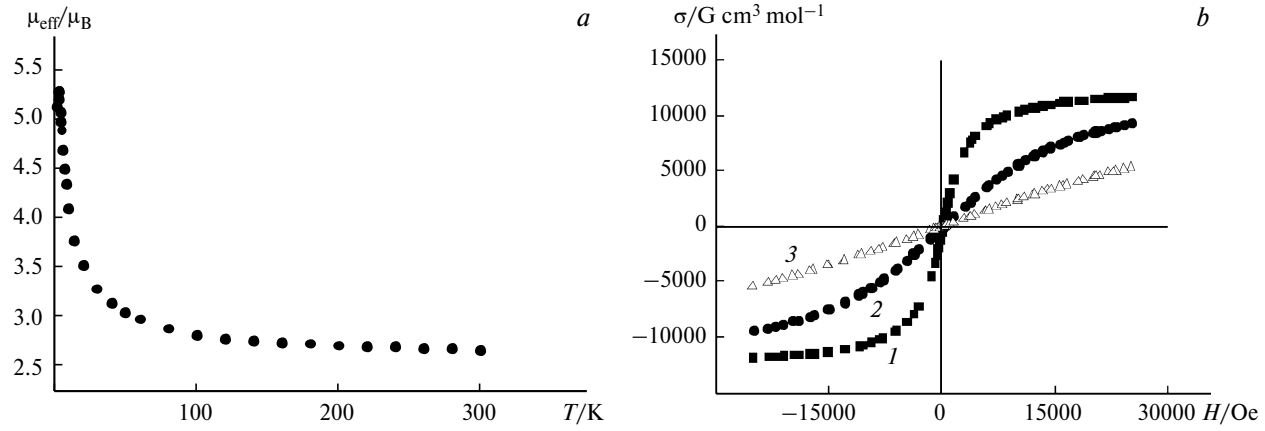

Fig. 4. Temperature dependence of the effective magnetic moment (μ_{eff}) (*a*) and the plots of the magnetization (σ) of the sample *versus* the external magnetic field (*H*) at $T = 2$ (*1*), 5 (*2*), and 9 K (*3*) (*b*) for the complex $[Cu(hfac)_2L]_n$.

100 to 300 K, the value of μ_{eff} remains constant (~3.5 μ_B). At temperatures below 100 K, μ_{eff} increases with decreasing temperature and reaches 4.94 μ_B at 5 K. At 2 K, the dependence of the magnetization of the sample on the applied field strength is nonlinear, which is indicative of the magnetic ordering. The spontaneous magnetization is 13049 G cm^3 mol^{-1}, which is somewhat smaller than the theoretical value (16755 G cm^3 mol^{-1}). The evaluation of the Curie temperature for $[Cu_2(hfac)_4L]_n$ gave $T_C \leq 2.5$ K.

The reaction of the nitronyl nitroxide L^{Me2} with $Cu(hfac)_2$ affords solid phases, which are also composed of the polymer chains $[Cu(hfac)_2L^{Me2}]_n$ and $[Cu_2(hfac)_4L^{Me2}]_n$. The heterospin complex $[Cu(hfac)_2L^{Me2}]_n$ crystallizes from toluene upon cooling. The complex $[Cu_2(hfac)_4L^{Me2}]_n$ was synthesized as described for $[Cu_2(hfac)_4L]_n$. The structure of the chain $[Cu_2(hfac)_4L^{Me2}]_n$ (Fig. 5, *a*) is similar to that of $[Cu_2(hfac)_4L]_n$ (see Fig. 3, *b*). In its coordination units, the Cu—O_{N-O} and Cu—N_{Iz} dis-

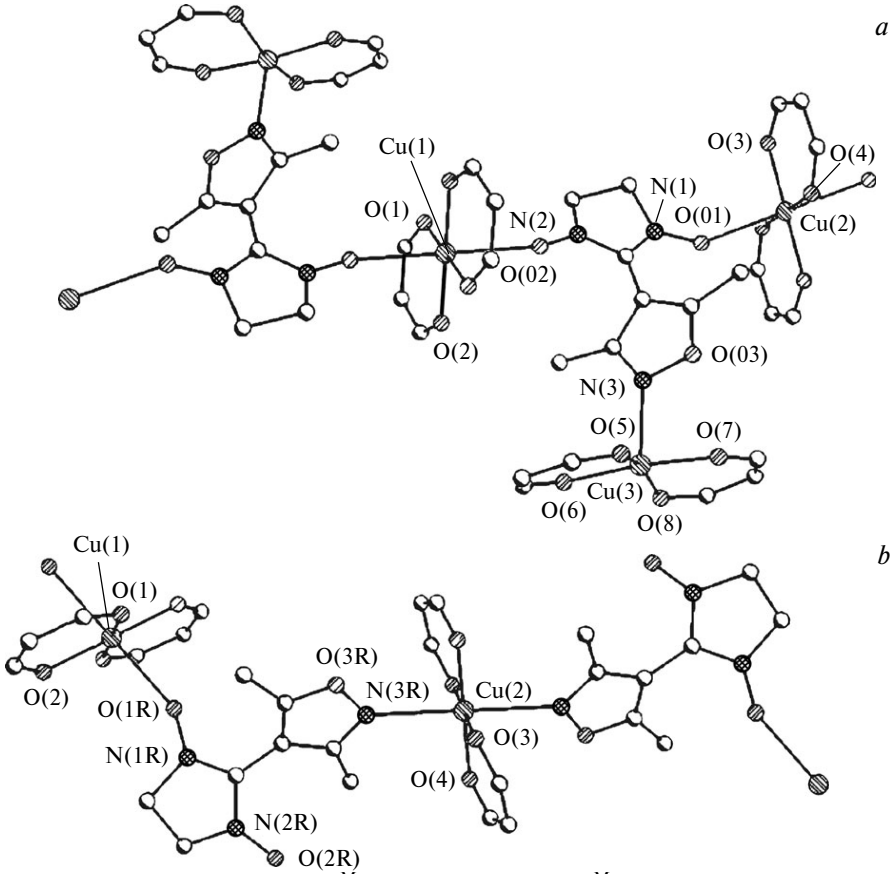

Fig. 5. Polymer chains in the structures of $[Cu_2(hfac)_4L^{Me2}]_n$ (*a*) and $[Cu(hfac)_2L^{Me2}]_n$ (*b*).

tances and the Cu—O—N angles are 2.487(2)—2.522(2) Å, 2.271(3) Å, and 146.5(2)—146.9(2)°, respectively, at 240 K, and these values change only slightly with a decrease in the temperature (see Table 2). The structure of the chain $[Cu(hfac)_2L^{Me2}]_n$ (see Fig. 5, *b*) is radically different from the above-described structure of $[Cu(hfac)_2L]_n$ (see Fig. 3, *a*). This chain is organized in a head-to-head manner. In this chain, two crystallographically independent Cu atoms are in different coordination environments. Thus, the centrosymmetric coordination square $\{Cu(hfac)_2\}$ around the Cu(1) atom is supplemented by two O atoms of the nitroxide groups ($d(Cu—O_{N—O})$ = 2.474(2) Å and Cu—O—N = 153.5(1)° at 240 K) to form an elongated octahedron, whereas the coordination environment of the Cu(2) atom involves two N_{Iz} atoms of two ligands L^{Me2} ($d(Cu—N_{Iz})$ = 2.503(2) Å). The geometric parameters change only slightly with a decrease in the temperature, except for the the distances between the noncoordinated O atoms of the NO groups of adjacent chains, which are 3.190 Å at 240 K and decrease to 3.159 Å at 55 K.

No other substantial structural changes, primarily, in the exchange clusters $\{ONCNO—Cu^{2+}—ONCNO\}$ within the polymer chains, are observed. This is a fundametally important result for the explanation of the temperature dependence of the effective magnetic moment of the complex $[Cu(hfac)_2L^{Me2}]_n$ (Fig. 6). If the cooling causes no substantial changes in the distances and angles in the exchange clusters $\{ONCNO—Cu^{2+}—ONCNO\}$, there are no thermally induced magnetic anomalies similar in character of the dependence $\mu_{eff}(T)$ to a spin-crossover,[1—28] as mentioned above. Supporting evidence for this conclusion is afforded by the fact that a slight change in the geometric parameters with a decrease in the temperature is inherent in both $[Cu(hfac)_2L^{Me2}]_n$ and $[Cu_2(hfac)_4L^{Me2}]_n$, whose effective magnetic moments do not decrease with decreasing temperature but, on the contrary, gradually increase, as in the case of the complex $[Cu(hfac)_2L]_n$ (see Fig. 4). Therefore, the results of the present study show that the decrease in the temperature causes only the thermal compression of the crystals of $[Cu(hfac)_2L^{Me2}]_n$ and $[Cu_2(hfac)_4L^{Me2}]_n$.

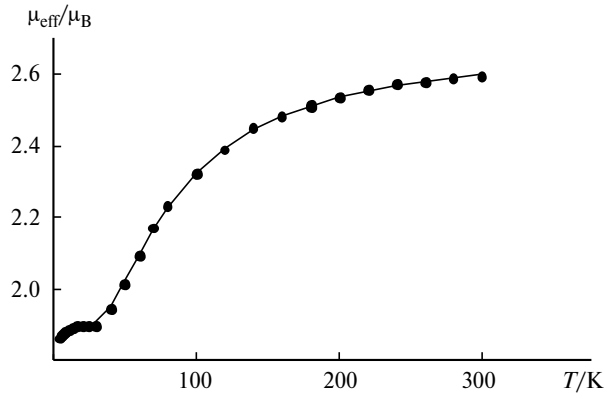

Fig. 6. Temperature dependence of the effective magnetic moment (μ_{eff}) for the complex $[Cu(hfac)_2L^{Me2}]_n$. The solid line represents the optimal theoretical curve with the parameters g_{Cu} = 2.37, g_R = 2.05, J/k = −54 K, zJ'/k = −1.3 K (the Hamiltonian $H = -2J(S_{1R}S_{Cu} + S_{2R}S_{Cu})$, the contribution of the single-spin cluster was taken into account according to the Curie law).

The magnetic properties of the complex $[Cu_2(hfac)_4L^{Me2}]_n$ are similar to those of the complex $[Cu_2(hfac)_4L]_n$. For the complex $[Cu(hfac)_2L^{Me2}]_n$, the effective magnetic moment is 2.59 μ_B at 300 K (see Fig. 6), which agrees well with the theoretical value of 2.45 μ_B for two noninteracting PMC with spins S = 1/2 and the *g*-factor of 2. As the temperature decreases, the magnetic moment μ_{eff} gradually decreases in the temperature range of 30—10 K and comes to a plateau (~1.90 μ_B), which corresponds to the theoretical value for one PMC with spin S = 1/2 and the *g*-factor of 2.19. This behavior of the dependence $\mu_{eff}(T)$ is indicative of fairly strong antiferromagnetic exchange interactions between PMC in the solid phase of the compound. As the temperatures decreases below 10 K, the magnetic moment μ_{eff} again decreases due to weak antiferromagnetic exchange interactions between the "residual" spins.

The strong antiferromagnetic exchange interaction in the structure of $[Cu(hfac)_2L^{Me2}]_n$ has two possible channels: intracluster and intercluster. In the case of the antiferromagnetic intracluster exchange nitroxide—nitroxide interaction ($\{ONCNO—Cu^{2+}—ONCNO\}$), the superexchange occurs through the atomic orbital d_{z^2} of the intracluster Cu^{2+} ion. The antiferromagnetic intercluster exchange nitroxide—nitroxide interaction ({ONCNO...ONCNO}) represents the direct exchange between the noncoordinated $O_{N—O}$ atoms of adjacent chains.[32] Taking into account the facts that the distances between the noncoordinated $O_{N—O}$ atoms of adjacent chains in $[Cu(hfac)_2L^{Me2}]_n$ are as short as 3.190 Å at 300 K and that these distances decrease to 3.159 Å upon cooling to 55 K (see Table 2), the decrease in the value of μ_{eff} in the temperature range of 30—300 K is, apparently, caused by the direct exchange interaction between the unpaired electrons of the paramagnetic ligands of adjacent chains (a similar situation has been observed earlier[33] in complexes with tetrazolyl-substituted nitronyl nitroxide radicals). Consequently, the exchange structure of $[Cu(hfac)_2L^{Me2}]_n$ can be considered as a system of weakly interacting two-center clusters. The approximation of the experimental dependence $\mu_{eff}(T)$ in terms of the isotropic spin-Hamiltonian ($H = -2JS_1S_2$) for the above-mentioned cluster[34] gave the optimal value of the exchange interaction between the unpaired electrons (J/k = −83 K). According to the results of quantum chemical calculations, the exchange interaction parameter is J/k = −93 K. Weaker antiferromagnetic exchange interactions, which are responsible for a slight decrease in μ_{eff} at temperatures below 10 K, are estimated at J'/k = −0.65 K.

It is worthy of note that the character of alternation of the bis-chelate fragments and the coordinated bridging spin-labeled ligands in the polymer chain and, consequently, the exchange clusters in the crystals of $[Cu(hfac)_2L^{Me_2}]_n$ are similar to those in compounds belonging to the family of "breathing" crystals.[6—9,12] For the latter, methods of analysis and interpretation of temperature-dependent ESR spectra are available.[13—17,20,32,35,36] The application of these approaches to the analysis of the ESR spectra of $[Cu(hfac)_2L^{Me_2}]_n$ provides additional information on the exchange interactions recorded by the static magnetic susceptibility method.

The ESR spectrum of a powder of $[Cu(hfac)_2L^{Me_2}]_n$ recorded at 20 K (Fig. 7, *a*) is well simulated as the superposition of the spectra for two types of PMC in a quantitative ratio of 1 : 1 (see Fig. 7, *c*). The first type corresponds to the single-spin site {N—Cu^{2+}—N}, *i.e.*, to the isolated Cu^{2+} ion, and is described by the *g*-tensor g_{Cu} = [2.058; 2.072; 2.340] and the component of the hyperfine coupling A_{ZZ}^{Cu} = 16 mT. The second type of sites corresponds to the three-spin cluster {ONCNO—Cu^{2+}—ONCNO} and is described by the *g*-tensor g_{RCuR} = [2.058; 2.061; 2.317] without a resolved hyperfine structure. The fact that at 20 K, the *g*-tensor of the three-spin cluster corresponds to the *g*-tensor of the Cu^{2+} ion is indicative of the strong antiferromagnetic exchange interaction between the unpaired electrons of PMC of the nitronyl nitroxide radicals.

The experimental spectrum of a powdered sample recorded at 300 K is also simulated as the superposition of the ESR spectra of two types of PMC but with a different quantitative ratio (1 : 3, see Fig. 7, *b*). The first type of sites, which we denote as {N—Cu^{2+}—N}, is described by almost the same magnetic-resonance parameters as at 20 K: g_{Cu} = [2.058; 2.072; 2.342], A_{ZZ}^{Cu} = 15.7 mT. The second type of sites, *viz.*, the exchange clusters {ONCNO—Cu^{2+}—ONCNO}, is characterized by the *g*-tensor g_{RCuR} = [2.03; 2.03; 2.11], whose principal values are close to the average value of the *g*-tensors of the Cu^{2+} ion (g_{Cu} = [2.058; 2.061; 2.317] at 20 K) and two nitronyl nitroxide radicals (g_R = 2.007). The fact that the ESR spectra measured at high (300 K) and low (20 K) temperatures show a resolved component of the hyper-

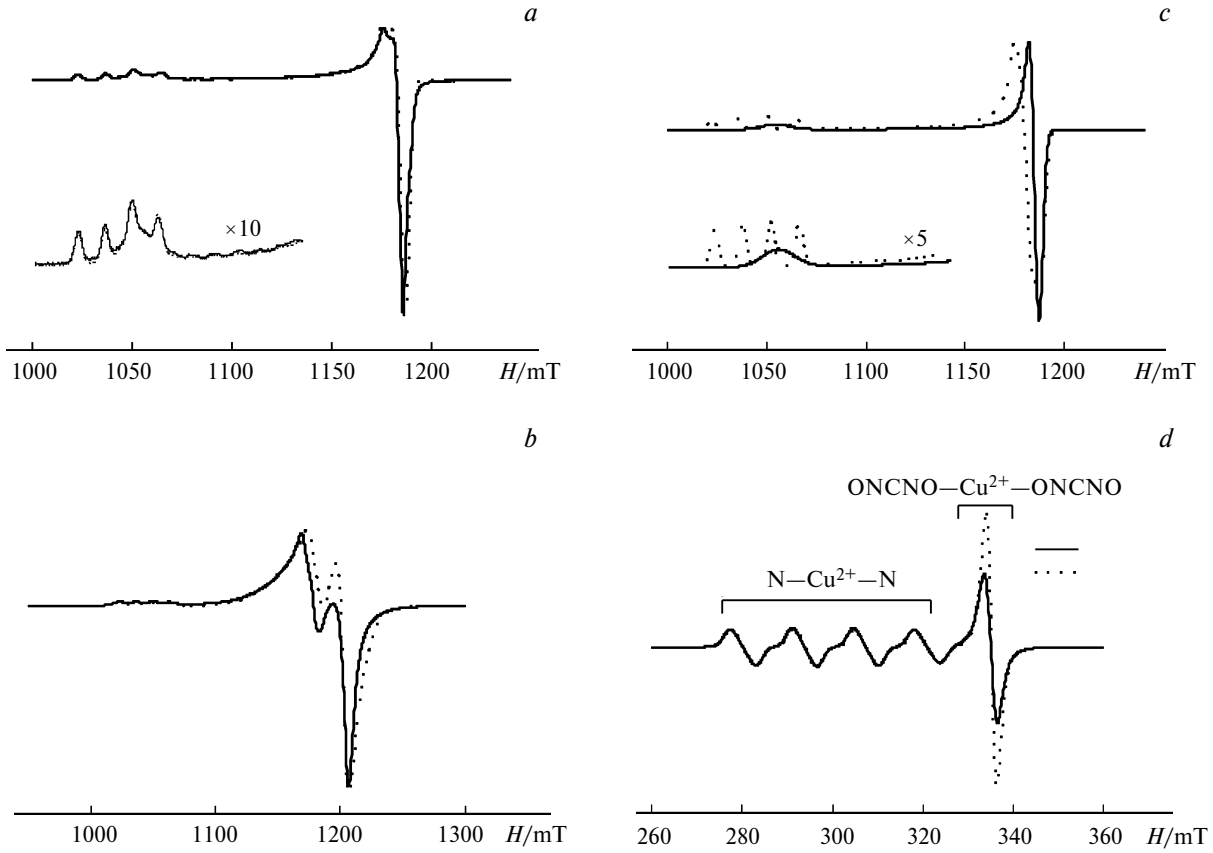

Fig. 7. Experimental (line) and calculated (points) ESR spectra of a polycrystalline sample of $[Cu(hfac)_2L^{Me_2}]_n$ at 20 (*a*) and 300 K (*b*). The parameters of the calculations: $\nu_{mw} \approx 34.18$ GHz, g_{RCuR} = [2.058; 2.061; 2.317], g_{Cu} = [2.058; 2.072; 2.340], A_{ZZ}^{RCuR} = 16 mT (*a*); $\nu_{mw} \approx 34.19$ GHz, g_{RCuR} = [2.030; 2.030; 2.110], g_{Cu} = [2.058; 2.072; 2.342], A_{ZZ}^{Cu} = 15.7 mT (*b*). The individual ESR spectra of the clusters {N—Cu^{2+}—N} (solid line) and {ONCNO—Cu^{2+}—ONCNO} (dashed line) used for the simulation of the spectra (*c*). The ESR spectra of a single crystal of $[Cu(hfac)_2L^{Me_2}]_n$ at 5 (solid line) and 20 K (dashed line), $\nu_{mw} \approx 9.75$ GHz; the spectra were normalized to the signal of {N—Cu^{2+}—N} (*d*).

fine coupling on the Cu^{2+} ion in {N—Cu^{2+}—N} with the splitting constant $A_{ZZ}^{Cu} \approx 16$ mT ≈ 0.016 cm^{-1} is indicative of the magnetic isolation of this ion and provides an estimate of its exchange interaction with adjacent PMC at $|J/k| << 0.016$ cm^{-1}.

Figure 7, *d* shows the ESR spectra of a single crystal of $[Cu(hfac)_2L^{Me_2}]_n$ measured at 5 and 20 K and normalized to the signal of the single-spin site {N—Cu^{2+}—N}. As the temperature decreases, the intensity of the ESR signal of the three-spin cluster {ONCNO—Cu^{2+}—ONCNO} substantially decreases compared to the intensity of the signal of the single-spin site {N—Cu^{2+}—N}. This is unambiguous evidence for the antiferromagnetic intercluster exchange interaction between the exchange clusters {ONCNO—Cu^{2+}—ONCNO} and confirms the conclusion[24,36] that the character of the temperature dependence typical of $[Cu(hfac)_2L^{Me_2}]_n$ in the range of 30—300 K is determined by the exchange interaction between the nitroxides of adjacent chains.

In the reaction of $Cu(hfac)_2$ with L^{Me_2}, we succeeded in isolating, in addition to the chain polymer complexes, the complexes $[Cu(hfac)_2L^{Me_2}_2]$ (Fig. 8, *a*) and $[Cu(hfac)_2L^{Me_2}(MeCN)]$ (Fig. 8, *b*) having a molecular structure. In the latter complexes, the paramagnetic ligand is coordinated through the N_{Iz} atom. The Cu—N_{Iz} distances in the centrosymmetric molecule $[Cu(hfac)_2L^{Me_2}_2]$ are 2.458(3) Å. The N atoms of acetonitrile and the isoxazole ring occupy the axial positions in the bipyramidal coordination environment of the central atom in the molecule $[Cu(hfac)_2L^{Me_2}(MeCN)]$; the Cu—$N_{Iz}$ and Cu—N_{MeCN} distances are 2.357(3) and 2.397(4) Å, respectively. In both structures, there are quite short O...O contacts between the uncoordinated nitroxide groups L^{Me_2} with the distances in the range of 3.340—3.483 Å (indicated by dashed lines, see Fig. 8, *c* and *d*).

For $[Cu(hfac)_2L^{Me_2}_2]$, the value of μ_{eff} (3.23 μ_B) remains virtually constant at temperatures ranging from 50 to 300 K (Fig. 9). As the temperature decreases below 50 K, μ_{eff} decreases and reaches 1.99 μ_B at 2 K. The value of μ_{eff} on the plateau is in good agreement with the theoretical value (3.0 μ_B) for three noninteracting PMC; the spin of each PMC is 1/2, and the *g*-factor is 2. The character of the dependence $\mu_{eff}(T)$ is indicative of the presence of weak antiferromagnetic interactions between the unpaired electrons of PMC, which is consistent with the X-ray diffraction data on the presence of contacts between the O atoms of the nitroxide groups of adjacent molecules in the crystal structure of $[Cu(hfac)_2L^{Me_2}_2]$ (as mentioned above, the interaction between the spins of the Cu^{2+} ions and nitroxides through the isoxazole ring is weak and can be ignored). The optimal exchange interaction parameter ($J/k = -3.5$ K) was estimated from the analysis of the dependence $\mu_{eff}(T)$ in terms of the uniform chain model for antiferromagnetically coupled PMC with spins $S = 1/2$ ($H = -2J\sum S_i S_{i+1}$) taking into account the contribution of Cu^{2+} ions to the magnetic susceptibility according to the Curie—Weiss law.

It was interesting to compare the magnetic properties of the Cu^{2+} compounds with the corresponding properties of the structurally similar Mn^{2+} compounds, which have

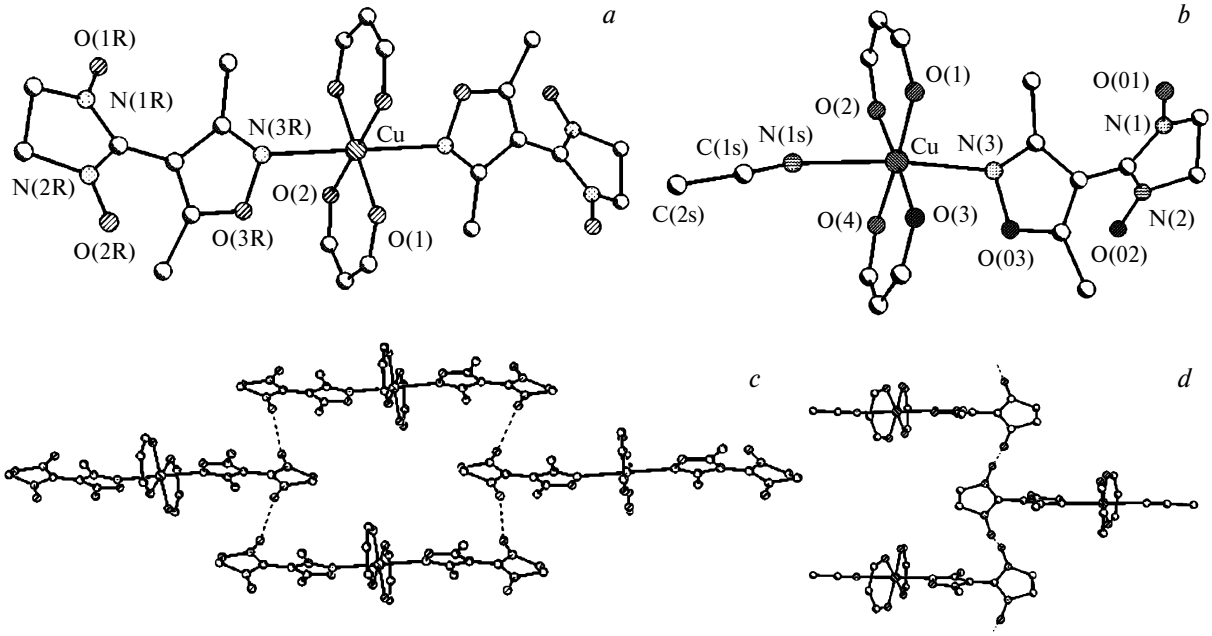

Fig. 8. Molecular structures of $[Cu(hfac)_2L^{Me_2}_2]$ (*a*) and $[Cu(hfac)_2L^{Me_2}(MeCN)]$ (*b*) and their crystal packing (*c*, *d*). Dashed lines indicate the shortest intermolecular O...O contacts.

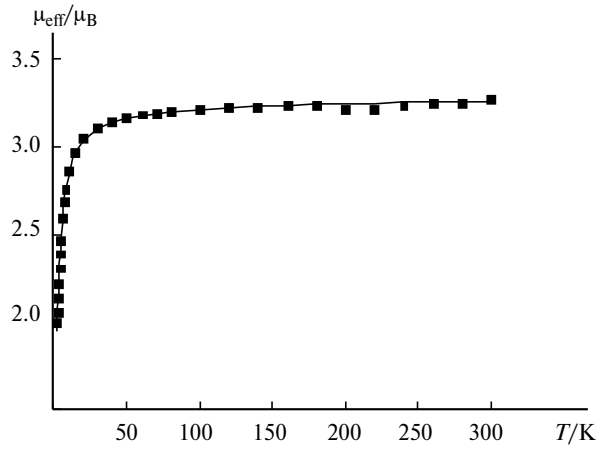

Fig. 9. Temperature dependence of the effective magnetic moment (μ_{eff}) for the complex $[Cu(hfac)_2L^{Me_2}{}_2]$. The solid line represents the optimal theoretical curve (see the comments in the text).

the spin of the ion metal ($S = 5/2$) maximum for d elements. However, we failed to isolate heterospin complexes isostructural to the above-described Cu^{2+} compounds. The reaction of $Mn(hfac)_2$ with L in a diethyl ether—hexane mixture afforded the trinuclear complex $[Mn_3(hfac)_6L_4]$. The reaction of $Mn(hfac)_2$ with L^{Me_2} in a diethyl ether—toluene mixture gave the dinuclear complex $[Mn(hfac)_2L^{Me_2}]_2$ as the solid phase.

In the centrosymmetric trinuclear molecule $[Mn_3(hfac)_6L_4]$, two ligands L are bidentate O,O´-bridging and are coordinated through the N—O groups (O(1b) and O(2b) atoms, see Fig. 10, *a*), thus binding the central and terminal Mn atoms ($d(Mn—O_{N—O})$ = 2.172(3) and 2.198(3) Å). Two other ligands L are coordinated to the terminal metal atoms (Mn(1)) in a monodentate fashion through the O(1a) atom ($d(Mn(1)—O_{N—O})$ = 2.134(3) Å) in the *cis* position with respect to the bridging ligands L. The intermolecular distances between the paramagnetic centers, *viz.*, the O atoms of the uncoordinated N—O groups, are longer than 4 Å. It should be noted that heterospin complexes of transition metals with nitronyl nitroxides having this structure have been unknown.[29] In the pseudocentrosymmetric molecule $[Mn(hfac)_2L^{Me_2}]_2$, the environment of each Mn atom is formed by four O atoms of two hfac ligands in *cis* positions with respect to each other, and the $O_{N—O}$ and N_{Iz} atoms (Mn—O_{hfac}, 2.103(2)—2.178(2) Å; Mn—$O_{N—O}$, 2.137(2) and 2.118(1) Å; Mn—N_{Iz}, 2.348(2) and 2.319(2) Å; Mn—O—N, 131.3(1) and 129.7(1)°) (Fig. 10, *b*). Taking into account the O...O distances between the O atoms of the N—O groups of adjacent dimers (3.321 and 3.908 Å), the packing of $[Mn(hfac)_2L^{Me_2}]_2$ can be considered as composed of chains of dimeric molecules (see Fig. 10, *c*).

The dependence $\mu_{eff}(T)$ for $[Mn(hfac)_2L^{Me_2}]_2$ is shown in Fig. 11, *a*. The magnetic moment μ_{eff} is 5.16 μ_B at 300 K. It decreases with decreasing temperature and comes to a plateau (~4.90 μ_B) in the temperature range of 80—200 K. Upon cooling to a temperature below 80 K, μ_{eff} first gradually decreases and then falls down to 2.48 μ_B at 2 K. The high-temperature value of μ_{eff} is substantially smaller than the theoretical spin-only value (6.16 μ_B) estimated by the summation of the contributions of two noninteracting PMC (the Mn^{2+} ion and the nitronyl nitroxide radical) to the magnetic susceptibility. The value of μ_{eff} on the plateau agrees well with the theoretical value (4.90 μ_B) characteristic of weakly interacting PMC with spin $S = 2$. As can be seen from the above data, strong antiferromagnetic exchange interactions between the spins of the Mn^{2+} ion ($S = 5/2$) and L^{Me_2} ($S = 1/2$) in $[Mn(hfac)_2L^{Me_2}]_2$ result in the partial compensation of the spins of Mn^{2+}. A decrease in μ_{eff} at $T < 80$ K is associated with weaker antiferromagnetic interactions between the dimers due to short contacts between the O atoms of the noncoordinated nitroxide groups. The analysis of the experimental dependence $\mu_{eff}(T)$ with the use of the isotropic Hamiltonian

$$H = -2J_1(S^1{}_{Mn}S^1{}_R + S^2{}_{Mn}S^2{}_R) - 2J_2(S^1{}_RS^2{}_R),$$

where J_1 is the parameter of the exchange interaction between the spins of the Mn^{2+} ion (S_{Mn}) and the nitronyl nitroxide radical (S_R) and J_2 is the parameter of the exchange interaction between the nitronyl nitroxide radicals, provides an estimate of the optimal values for the parameters J_1 and J_2 and the g-factor, which are −109(±4) K, −1.13(±0.02) K, and 2.005(±0.007), respectively.

For $[Mn_3(hfac)_6L_4]$, the high-temperature value of μ_{eff} is 10.26 μ_B (see Fig. 11, *b*). Upon cooling, μ_{eff} gradually increases up to 12.10 μ_B at 30 K and then falls down to 9.20 μ_B at 2 K. The value of μ_{eff} at 300 K is somewhat smaller than the theoretical spin-only value (10.82 μ_B) estimated by the summation of the contributions of seven noninteracting PMC (three of which have spin $S = 5/2$ and four have spin $S = 1/2$) to the magnetic susceptibility. Therefore, strong antiferromagnetic exchange interactions between the spins of the Mn^{2+} ions and the nitronyl nitroxide radicals are developed both in $[Mn_3(hfac)_6L_4]$ and $[Mn(hfac)_2L^{Me_2}]_2$. The maximum value of μ_{eff}, which is equal to 12.10 μ_B at 30 K, is close to the theoretical value (11.96 μ_B) on the assumption that the spins of the nitroxides partially compensate the spins of the Mn^{2+} ions, and the residual spins are ferromagnetically coupled. The presence of fairly strong ferromagnetic exchange interactions is evidenced by an increase in μ_{eff} with temperature decreasing from 300 to 30 K. Weaker intermolecular exchange interactions appear at temperatures below 30 K, resulting in a decrease in μ_{eff}.

Therefore, we synthesized and characterized the first heterospin complexes $Cu(hfac)_2$ and $Mn(hfac)_2$ with new stable 2-imidazoline radicals, *viz.*, spin-labeled isoxazole derivatives L and L^{Me_2}. It was found that the weak elec-

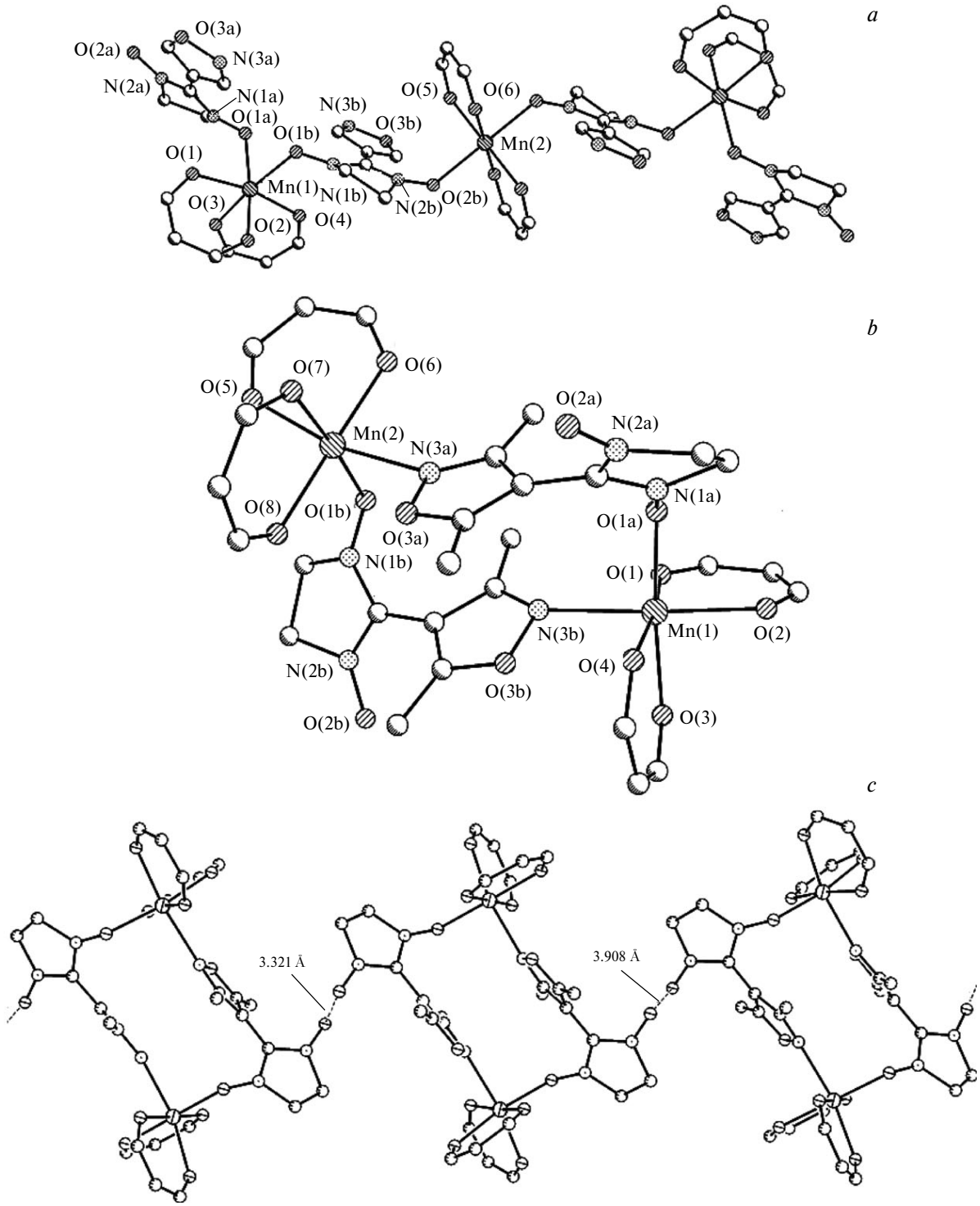

Fig. 10. Molecular structures of $[Mn_3(hfac)_6L_4]$ (*a*) and $[Mn(hfac)_2L^{Me_2}]_2$ (*b*) and the packing of dimers in $[Mn(hfac)_2L^{Me_2}]_2$ (*c*).

tron-donating ability of the N and O atoms of the isoxazole ring L does not allow them to coordinate the metal ion. An increase in the electron-donating properties of the N atom of the isoxazole ring due to the introduction of two methyl substituents into the aromatic ring leads to the formation of heterospin complexes through the coordination of this N atom, including the chain polymer complex, in which the bidentate-bridging ligand L^{Me_2} is coordinated through both the O atom of the nitroxide group and the N atom of the isoxazole ring.

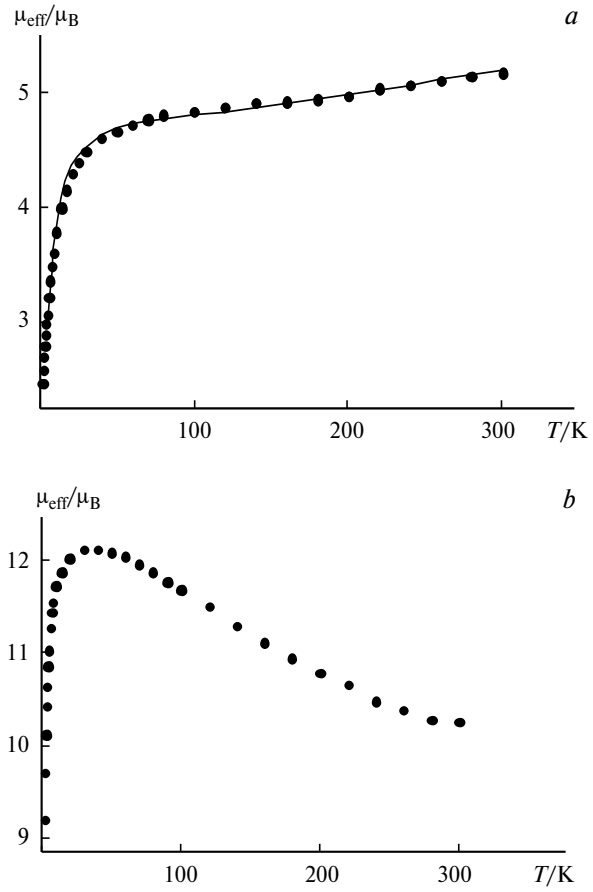

Fig. 11. Temperature dependences of the effective magnetic moment (μ_{eff}) for the complexes $[Mn(hfac)_2L^{Me_2}]_2$ (*a*) and $[Mn_3(hfac)_6L_4]$ (*b*). The solid line indicates the optimal theoretical curve with the parameters $J_1 = -109$ K, $J_2 = -1.13$ K, and $g = 2.005$.

The study of the magnetic properties of $[Cu(hfac)_2L]_n$, $[Cu_2(hfac)_4L]_n$, and $[Cu_2(hfac)_4L^{Me_2}]_n$ in the temperature range of 2—300 K revealed ferromagnetic ordering at temperatures below 5 K. An analysis of the ESR spectra and the dependence $\mu_{eff}(T)$ for $[Cu(hfac)_2L^{Me_2}]_n$ showed that a decrease in the magnetic moment with temperature decreasing from 300 to 30 K is a consequence of interchain antiferromagnetic exchange interactions between the paramagnetic fragments of the nitronyl nitroxide radicals. The subsequent decrease in the magnetic moment in the temperature range of 20—4 K is due to exchange interactions between the Cu^{2+} ions of the exchange clusters {ONCNO—Cu^{2+}—ONCNO} of adjacent chains.

It was found that the reaction of $[Mn(hfac)_2]$ with L or L^{Me_2} affords compounds having a different structure of the heterospin molecules than in the case of the reaction of $[Cu(hfac)_2]$ with L or L^{Me_2}. Noteworthy is the structure of the trinuclear complex $[Mn_3(hfac)_6L_4]$, which has not been observed earlier among heterospin transition metal complexes with nitronyl nitroxide radicals.

Experimental

4-Iodoisoxazole,[37] 3,5-dimethyl-4-iodoisoxazole,[38] and 2,3-bis(hydroxylamino)-2,3-dimethylbutane[39] were synthesized according to known procedures. Commercial reagents and solvents were used as is. The chromatography was performed with the use of Silica Gel 60 F_{254} TLC aluminum sheets and 0.063—0.200 mm silica gel (for column chromatography, Merck). The IR spectra were recorded in KBr pellets on a VECTOR-22 spectrophotometer (Bruker). The melting points were determined on a BOETIUS micro hot-stage apparatus. Microanalyses were carried out in the N. N. Vorozhtsov Novosibirsk Institute of Organic Chemistry of the Siberian Branch of the Russian Academy of Sciences on an EURO EA3000 CHNS analyzer. Magnetochemical measurements were performed on a Quantum Design MPMS*XL* SQUID magnetometer in the temperature range of 2—300 K. The effective magnetic moments were calculated from the equation

$$\mu_{eff}(T) = (8\chi'_M T)^{1/2},$$

where χ'_M is the molar paramagnetic component of the magnetic susceptibility estimated with the use of Pascal constants.[40] The steady-state X-band ESR spectra of 10^{-5} *M* solutions of the nitroxides L and L^{Me_2} in toluene were recorded at room temperature on a Bruker EMX spectrometer and were simulated with the use of the WINSIM v.0.96 program package.[41] The isotropic *g*-factors were determined with the use of solid diphenylpicrylhydrazyl as the reference; the accuracy of the determination of the hyperfine coupling constants and the *g*-factors was 0.005 mT and 0.0001, respectively. The ESR spectrum of a polycrystalline sample of $[Cu(hfac)_2L^{Me_2}]_n$ was recorded in the continuous-wave (CW) mode on a Bruker ELEXSYS E580 spectrometer equipped with an Oxford Instruments thermostat ($T = 4$—300 K).

Quantum chemical calculations were carried out with the ORCA program[42] using the the PBE0 hybrid functional[43] in the broken-symmetry approach.[44—46] The 6-31G(d) basis set[47] was employed for the C, N, O, and H atoms. All calculations were performed based on the X-ray diffraction data for $[Cu(hfac)_2L^{Me_2}]_n$ obtained at 55 K without any specific modification or optimization.

2-(3,5-Dimethylisoxazol-4-yl)-4,4,5,5-tetramethylimidazolidine-1,3-diol (4b). A 1.6 *M* BuLi solution in hexane (2.3 mL, 3.7 mmol) was added to a solution of 3,5-dimethyl-4-iodoisoxazole (0.8 g, 3.6 mmol) in THF (20 mL) stirred at −90 °C under argon. After 20 min, ethyl formate (0.29 g, 3.9 mmol) was added. The reaction mixture was stirred for 0.5 h. Then the cooling was stopped, and a solution of H_2SO_4 (0.5 mL) in THF (10 mL) was added. After 10 min, an aqueous $NaHCO_3$ solution was added to neutralize the excess acid. The product was extracted with CH_2Cl_2, and the extracts were combined, dried over Na_2SO_4, and concentrated. The resulting crude aldehyde was dissolved in MeOH (10 mL), bis(hydroxylamine) **3** (0.53 g, 3.6 mmol) was added, and the mixture was stirred for 12 h and then kept at 0 °C for 3 h. The precipitate that formed was filtered off, washed with toluene, and dried. Yield 0.21 g (16%). IR, ν/cm^{-1}: 467, 500, 620, 752, 842, 918, 1001, 1026, 1047, 1118, 1143, 1266, 1362, 1424, 1642, 2936, 2982, 3330, 3547. Found (%): C, 56.5; H, 8.3; N, 16.6. $C_{12}H_{21}N_3O_3$. Calculated (%): C, 56.5; H, 8.3; N, 16.5.

2-(3,5-Dimethylisoxazol-4-yl)-4,4,5,5-tetramethyl-4,5-dihydro-1*H*-imidazole-3-oxide-1-oxyl (L^{Me_2}). Sodium periodate

Table 3. Crystallographic characteristics and the X-ray data collection statistics for the ligands L and L^{Me_2} and their molecular complexes

Parameter	L	L^{Me_2}	$[Cu(hfac)_2L^{Me_2}_2]$	$[Cu(hfac)_2L^{Me_2}\cdot(MeCN)]$	$[Mn(hfac)_2L^{Me_2}]_2$	$[Mn_3(hfac)_6L_4]$
M	224.24	252.29	982.24	771.00	1442.70	2304.14
T/K	298	240	240	295	240	240
Space group	$C2/c$	$P\bar{1}$	$P\bar{1}$	$P2_1/c$	$P\bar{1}$	$P\bar{1}$
Z	4	2	2	4	2	2
a/Å	11.343(5)	7.922(5)	9.708(4)	13.5637(15)	11.2222(9)	9.5394(19)
b/Å	9.880(4)	9.802(6)	10.207(4)	9.7047(9)	15.0156(12)	15.485(3)
c/Å	11.041(4)	9.846(6)	12.437(5)	24.168(3)	20.0174(15)	17.276(4)
α/deg	—	75.679(11)	109.086(6)	—	69.349(5)	108.576(15)
β/deg	109.868(6)	67.006(10)	111.778(6)	92.813(5)	82.268(5)	92.698(15)
γ/deg	—	69.443(10)	92.969(6)	—	72.791(5)	100.503(16)
V/Å^3	1163.7(8)	653.6(7)	1060.3(8)	3177.5(6)	3013.3(4)	2363.4(8)
d_{calc}/g cm^{-3}	1.280	1.282	1.538	1.612	1.590	1.619
μ/mm^{-1}	0.096	0.093	0.628	0.805	0.556	0.540
θ-Angle range/deg	2.81—23.36	2.24—26.45	1.90—26.48	1.50—28.32	1.09—28.06	2.18—26.46
Number of measured /independent reflections	4411/845	4241/2659	10677/4345	27577/7810	47443/14261	16041/9562
R_{int}	0.0523	0.0704	0.0813	0.1218	0.0521	0.1041
N	103	238	340	515	965	766
GOOF	1.058	0.928	1.109	0.709	0.791	0.941
R_1	0.0387	0.0489	0.0485	0.0461	0.0397	0.0756
wR_2 ($I > 2\sigma(I)$)	0.1091	0.1043	0.1155	0.0811	0.0815	0.1722
R_1	0.0467	0.0750	0.0699	0.1678	0.1182	0.1355
wR_2 (based on all reflections)	0.1153	0.1148	0.1393	0.1009	0.0978	0.2082

$NaIO_4$ (0.24 g, 1.1 mmol) was added portionwise during 0.5 h to a mixture of compound **4b** (0.19 g, 0.75 mmol), $CHCl_3$ (15 mL), and H_2O (5 mL) stirred at +5 °C. Then the organic layer was separated, dried over Na_2SO_4, concentrated to ~3 mL, and applied on a column with SiO_2 (1.5×20 cm, ethyl acetate as the eluent). The blue fraction was concentrated, and the residue was crystallized from a CH_2Cl_2—heptane mixture. Yield 0.16 g (85%), m.p. 172—174 °C. IR, ν/cm^{-1}: 469, 541, 615, 755, 819, 866, 1048, 1147, 1165, 1228, 1267, 1361, 1397, 1454, 1645, 2988, 3425. ESR: g_{iso} = 2.0066, $a_{N(N-O)}$(2 N) = 0.722 mT, $a_{H(Me)}$(12 H) = 0.02 mT, a_H(2 H) = 0.05 mT, a_N(2 N) = 0.03 mT*. Found (%): C, 57.4; H, 7.4; N, 17.1. $C_{13}H_{19}N_4O_4$. Calculated (%): C, 57.1; H, 7.2; N, 16.7.

4,4,5,5-Tetramethyl-2-(isoxazol-4-yl)-4,5-dihydro-1*H*-imidazole-3-oxide-1-oxyl (L) was synthesized as described for the ligand L^{Me_2}. Total yield 18%, m.p. 120—121 °C. IR, ν/cm^{-1}: 466, 539, 589, 657, 748, 826, 870, 907, 1004, 1125, 1177, 1209, 1223, 1324, 1374, 1409, 1424, 1455, 1620, 2983, 3131. ESR: g_{iso} = 2.0065, $a_{N(N-O)}$(2 N) = 0.745 mT, $a_{H(Me)}$(12 H) = 0.02 mT, a_H(1 H) = 0.065 mT, a_H(1 H) = 0.042 mT, a_N(2 N) = 0.03 mT*. Found (%): C, 53.6; H, 6.6; N, 18.6. $C_{13}H_{19}N_4O_4$. Calculated (%): C, 53.6; H, 6.3; N, 18.7.

Catena{(μ_2-4,4,5,5-tetramethyl-2-(isoxazol-4-yl)-4,5-dihydro-1*H*-imidazole-3-oxide-1-oxyl-*O*,*O*)bis(1,1,1,5,5,5-hexafluoropentane-2,4-dionato)copper} ($[Cu(hfac)_2L]_n$). Hexane (3 mL) was added to a solution of $Cu(hfac)_2$ (0.04 g, 0.08 mmol) and L (0.0188 g, 0.08 mmol) in CH_2Cl_2 (2 mL). After the storage of the reaction mixture in the open flask for 24 h, blue-violet crystals formed. The crystals were filtered off, washed with cold hexane, and dried in air. Yield 58%. Found (%): C, 34.7; H, 2.5; F, 32.6; N, 5.8. $C_{20}H_{16}CuF_{12}N_3O_7$. Calculated (%): C, 34.2; H, 2.3; F, 32.5; N, 6.0.

Bis[2-(3,5-dimethylisoxazol-4-yl)-4,4,5,5-tetramethyl-4,5-dihydro-1*H*-imidazole-3-oxide-1-oxyl]bis(1,1,1,5,5,5-hexafluoropentane-2,4-dionato)copper ($[Cu(hfac)_2L^{Me_2}_2]$). Hexane (5 mL) was added to a solution of $Cu(hfac)_2$ (0.0379 g, 0.08 mmol) and L^{Me_2} (0.04 g, 0.16 mmol) in CH_2Cl_2 (3 mL). The reaction mixture was kept in an open flask at −18 °C for 40 h. The elongated dark blue crystals that formed were filtered off, washed with cold hexane, and dried in air. Yield 95%. Found (%): C, 41.3; H, 3.9; F, 23.7; N, 8.4. $C_{34}H_{38}CuF_{12}N_6O_{10}$. Calculated (%): C, 41.6; H, 3.9; F, 23.2; N, 8.6. This complex can be prepared with the use of the reagents taken in any ratio by crystallization from diethyl ether.

Catena{(μ_2-2-(3,5-dimethylisoxazol-4-yl)-4,4,5,5-tetramethyl-4,5-dihydro-1*H*-imidazole-3-oxide-1-oxyl-*N*,*O*)bis(1,1,1,5,5,5-hexafluoropentane-2,4-dionato)copper} ($[Cu(hfac)_2L^{Me_2}]_n$). A solution of $Cu(hfac)_2$ (0.0379 g, 0.08 mmol) and L^{Me_2} (0.02 g, 0.08 mmol) in toluene (5 mL) was concentrated to ~2 mL by

* In order to reproduce the line shape of the multiplets in the simulated ESR spectra of L and L^{Me_2}, we had to introduce small hyperfine coupling constants with the nuclei of the H and N atoms of the isoxazole ring apart from the hyperfine coupling of the unpaired electron with two nuclei of the N atoms of the imidazoline ring and 12 nuclei of the H atoms of the methyl groups.

Table 4. Crystallographic characteristics and the X-ray data collection statistics for the complexes $[Cu(hfac)_2L]_n$ and $[Cu_2(hfac)_4L]_n$

Parameter	$[Cu(hfac)_2L]_n$	$[Cu_2(hfac)_4L]_n$
M	701.90	1179.55
T/K	295	240
Space group	$P\bar{1}$	$P\bar{1}$
Z	2	2
a/Å	9.5497(3)	12.0937(11)
b/Å	9.8247(3)	13.3086(14)
c/Å	16.5530(5)	15.6413(15)
α/deg	78.060(2)	68.442(6)
β/deg	76.178(2)	69.545(6)
γ/deg	77.737(2)	80.584(7)
V/Å^3	1453.58(8)	2191.9(4)
d_{calc}/g cm^{-3}	1.604	1.787
μ/mm^{-1}	0.870	1.129
θ-Angle range/deg	2.15—27.60	1.48—28.02
Number of measured /independent reflections	23318/6645	37898/10441
R_{int}	0.0375	0.0774
N	499	662
GOOF	0.907	1.006
R_1	0.0449	0.0790
wR_2 ($I > 2\sigma(I)$)	0.1268	0.2605
R_1	0.0887	0.1513
wR_2 (based on all reflections)	0.1411	0.2813

blowing with air at a low flow rate and then kept at 5 °C for 24 h. The dark brown crystals that formed were filtered off, washed with cold toluene, and dried in air. Yield 72%. Found (%): C, 36.5; H, 3.0; F, 31.8; N, 5.6. $C_{22}H_{20}CuF_{12}N_3O_7$. Calculated (%): C, 36.2; H, 2.8; F, 31.2; N, 5.8. The storage of the reaction mixture for one weak in the presence of MeCN vapor at −18 °C afforded dark blue crystals of the composition $[Cu(hfac)_2L^{Me_2}(MeCN)]$. Yield 35%. Found (%): C, 37.7; H, 3.0; F, 29.5; N, 7.3. $C_{24}H_{23}CuF_{12}N_4O_7$. Calculated (%): C, 37.4; H, 3.0; F, 29.6; N, 7.3.

Catena{(μ$_3$-2-(3,5-dimethylisoxazol-4-yl)-4,4,5,5-tetramethyl-4,5-dihydro-1*H*-imidazole-3-oxide-1-oxyl-*N*,*O*,*O*)bis[bis(1,1,1,5,5,5-hexafluoropentane-2,4-dionato)copper]} ($[Cu_2(hfac)_4L^{Me_2}]_n$). The compounds $Cu(hfac)_2$ (0.0757 g, 0.16 mmol) and L^{Me_2} (0.02 g, 0.08 mmol) were dissolved with heating in hexane (20 mL). The resulting solution was cooled to room temperature for 2 h. The intergrowths of dark brown crystals that formed were filtered off, washed with cold hexane, and dried in air. Yield 51%. Found (%): C, 31.3; H, 2.1; F, 38.4; N, 3.2. $C_{32}H_{22}F_{24}Cu_2N_3O_{11}$. Calculated (%): C, 31.8; H, 1.8; F, 37.8; N, 3.5.

Catena{(μ$_3$-4,4,5,5-tetramethyl-2-(isoxazol-4-yl)-4,5-dihydro-1*H*-imidazole-3-oxide-1-oxyl-*N*,*O*,*O*)bis[bis(1,1,1,5,5,5-hexafluoropentane-2,4-dionato)copper]} ($[Cu_2(hfac)_4L]_n$) was synthesized as described above. Dark brown crystals were obtained. Yield 49%. Found (%): C, 31.0; H, 1.8; F, 38.2; N, 3.5. $C_{30}H_{18}Cu_2F_{24}N_3O_{11}$. Calculated (%): C, 30.6; H, 1.5; F, 38.7; N, 3.6.

Tetrakis[4,4,5,5-tetramethyl-2-(isoxazol-4-yl)-4,5-dihydro-1*H*-imidazole-3-oxide-1-oxyl]tris[bis(1,1,1,5,5,5-hexafluoropentane-2,4-dionato)manganese] ($[Mn(hfac)_2]_3L_4$). Hexane

Table 5. Crystallographic characteristics and the X-ray data collection statistics for the complexes $[Cu_2(hfac)_4L^{Me_2}]_n$ and $[Cu(hfac)_2L^{Me_2}]_n$ at different temperatures

Parameter	$[Cu_2(hfac)_4L^{Me_2}]_n$		$[Cu(hfac)_2L^{Me_2}]_n$			
	47 K	240 K	55 K	100 K	150 K	240 K
M	603.80	603.80	729.95	729.95	729.95	729.95
Space group	$P\bar{1}$	$P\bar{1}$	$P\bar{1}$	$P\bar{1}$	$P\bar{1}$	$P\bar{1}$
Z	2	2	2	2	2	2
a/Å	11.8915(7)	12.1166(8)	9.1439(5)	9.1524(5)	9.1696(7)	9.194(5)
b/Å	13.5008(9)	13.6844(8)	11.3037(6)	11.3386(5)	11.4047(8)	11.528(6)
c/Å	16.0654(10)	16.2110(9)	13.8564(7)	13.8884(7)	13.9321(9)	13.977(8)
α/deg	70.971(4)	72.207(3)	82.146(3)	82.044(3)	81.938(4)	81.795(9)
β/deg	70.133(3)	69.928(3)	87.870(3)	87.842(3)	87.860(5)	87.787(10)
γ/deg	83.055(4)	84.605(3)	80.158(3)	80.180(3)	80.201(5)	79.924(9)
V/Å^3	2293.0(2)	2403.7(3)	1397.74(13)	1406.34(12)	1421.39(17)	1443.5(14)
d_{calc}/g cm^{-3}	1.749	1.668	1.734	1.724	1.706	1.679
μ/mm^{-1}	1.081	1.031	0.909	0.903	0.893	0.88
θ-Angle range/deg	1.60—28.41	1.56—28.25	2.21—28.33	2.20—28.32	2.25—28.12	2.17—29.60
Number of measured /independent reflections	24443/11002	40241/11551	20525/6782	20257/6819	15477/6742	17066/7362
R_{int}	0.0488	0.0512	0.0565	0.0512	0.0483	0.0805
N	689	752	492	474	492	510
GOOF	1.093	1.011	1.076	1.009	0.963	0.827
R_1	0.0548	0.0500	0.0354	0.0354	0.0397	0.0498
wR_2 ($I > 2\sigma(I)$)	0.1470	0.1477	0.0885	0.0901	0.0933	0.0937
R_1	0.0832	0.0897	0.0434	0.0453	0.0560	0.0924
wR_2 (based on all reflections)	0.1555	0.1592	0.0912	0.0933	0.0985	0.1067

(2 mL) was added to a solution of $Mn(hfac)_2(H_2O)_2$ (0.05 g, 0.1 mmol) and L (0.0222 g, 0.10 mmol) in diethyl ether (3 mL). The reaction mixture was kept in the open flask at −18 °C for 70 h. Platelet crystals that formed were filtered off, washed with cold toluene, and dried in air. Yield 73%. Found (%): C, 36.8; H, 2.7; F, 29.1; N, 7.1. $C_{70}H_{62}F_{36}Mn_3N_{12}O_{24}$. Calculated (%): C, 36.5; H, 2.7; F, 29.7; N, 7.3.

Bis[μ_2-2-(3,5-dimethylisoxazol-4-yl)-4,4,5,5-tetramethyl-4,5-dihydro-1*H*-imidazole-3-oxide-1-oxyl-*N*,*O*]bis(1,1,1,5,5,5-hexafluoropentane-2,4-dionato)manganese ($[Mn(hfac)_2L^{Me_2}]_2$). A solution of $Mn(hfac)_2(H_2O)_2$ (0.04 g, 0.08 mmol) in diethyl ether (2 mL) was added to a solution of L^{Me_2} (0.02 g, 0.08 mmol) in toluene (5 mL). After the storage of the reaction mixture in the open flask at −18 °C for 40 h, crystals precipitated. The crystals were filtered off, washed with cold toluene, and dried in air. Yield 37%. Found (%): C, 36.2; H, 2.3; F, 31.4; N, 5.5. $C_{44}H_{40}F_{24}Mn_2N_6O_{14}$. Calculated (%): C, 36.6; H, 2.8; F, 31.6; N, 5.8.

X-ray diffraction study. Single-crystal X-ray diffraction data sets were collected on a SMART APEX II CCD diffractometer (Bruker AXS) equipped with an Oxford Cryosystems Helix low-temperature attachment (Mo-Kα, λ = 0.71073 Å, absorption corrections were applied using the Bruker SADABS software, version 2.10). The structures were solved by direct methods and refined by the full-matrix least-squares method with anisotropic displacement parameters for all nonhydrogen atoms. The hydrogen atoms were positioned geometrically and refined using a riding model. All calculations associated with the structure solution and refinement were carried out with the use of the Bruker Shelxtl software, Version 6.14. Selected bond lengths are listed in Tables 1 and 2. Crystallographic parameters and the X-ray diffraction data collection and refinement statistics are given in Tables 3—5.

We thank D. V. Stass for recording and analyzing the ESR spectra.

This study was financially supported by the Russian Foundation for Basic Research (Project Nos 09-03-00091 and 11-03-00027), the Council on Grants at the President of the Russian Federation (Program for State Support of Young Scientists, Grants MK-4268.2010.3 and MK-868.2011.3), the Russian Academy of Sciences, and the Siberian Branch of the Russian Academy of Sciences.

References

1. F. Lanfranc de Panthou, E. Belorizky, R. Calemczuk, D. Luneau, C. Marcenat, E. Ressouche, P. Turek, P. Rey, *J. Am. Chem. Soc.*, 1995, **117**, 11247.
2. G. V. Romanenko, K. Yu. Maryunina, A. S. Bogomyakov, R. Z. Sagdeev, V. I. Ovcharenko, *Inorg. Chem.*, 2011, **50**, 6597.
3. F. Iwahory, K. Inoue, H. Iwamura, *Mol. Cryst. Liq. Cryst.*, 1999, **334**, 533.
4. A. Caneschi, P. Chiesi, L. David, F. Ferraro, D. Gatteschi, R. Sessoli, *Inorg. Chem.*, 1993, **32**, 1445.
5. M. Baskett, P. M. Lahti, A. Paduan-Filho, N. F. Jr. Oliveira, *Inorg. Chem.*, 2005, **44**, 6725.
6. V. I. Ovcharenko, S. V. Fokin, G. V. Romanenko, Yu. G. Shvedenkov, V. N. Ikorskii, E. V. Tret´yakov, S. F. Vasilevskii, *Zh. Strukt. Khim.,* 2002, **43**, 163 [*Russ. J. Struct. Chem. (Engl. Transl.)*, 2002, **43**, 153].
7. V. I. Ovcharenko, S. V. Fokin, G. V. Romanenko, V. N. Ikorskii, E. V. Tretyakov, S. F. Vasilevsky, R. Z. Sagdeev, *Mol. Phys.*, 2002, **100**, 1107.
8. P. Rey, V. I. Ovcharenko, in *Magnetism: Molecules to Materials, IV*, Eds J. S. Miller, M. Drillon, Wiley—VCH, New York, 2003, 41.
9. V. I. Ovcharenko, K. Yu. Maryunina, S. V. Fokin, G. V. Romanenko, V. N. Ikorskii, *Izv. Akad. Nauk, Ser. Khim.*, 2004, 2305 [*Russ. Chem. Bull., Int. Ed.*, 2004, **53**, 2406].
10. S. Fokin, V. Ovcharenko, G. Romanenko, V. Ikorskii, *Inorg. Chem.*, 2004, **43**, 969.
11. K. Maryunina, S. Fokin, V. Ovcharenko, G. Romanenko, V. Ikorskii, *Polyhedron*, 2005, **24**, 2094.
12. V. I. Ovcharenko, G. V. Romanenko, K. Yu. Maryunina, A. S. Bogomyakov, E. V. Gorelik, *Inorg. Chem.*, 2008, **47**, 9537.
13. M. Fedin, S. Veber, I. Gromov, V. Ovcharenko, R. Sagdeev, A. Schweiger, E. Bagryanskaya, *J. Phys. Chem. A*, 2006, **110**, 2315.
14. M. Fedin, S. Veber, I. Gromov, V. Ovcharenko, R. Sagdeev, E. Bagryanskaya, *J. Phys. Chem. A*, 2007, **111**, 4449.
15. M. Fedin, S. Veber, I. Gromov, K. Maryunina, S. Fokin, G. Romanenko, R. Sagdeev, V. Ovcharenko, E. Bagryanskaya, *Inorg. Chem.*, 2007, **46**, 11405.
16. S. L. Veber, M. V. Fedin, A. I. Potapov, K. Yu. Maryunina, G. V. Romanenko, R. Z. Sagdeev, V. I. Ovcharenko, D. Goldfarb, E. G. Bagryanskaya, *J. Am. Chem. Soc.*, 2008, **130**, 2444.
17. S. L. Veber, M. V. Fedin, G. V. Romanenko, R. Z. Sagdeev, E. G. Bagryanskaya, V. I. Ovcharenko, *Inorg. Chim. Acta*, 2008, **361**, 4148.
18. M. Fedin, V. Ovcharenko, E. Bagryanskaya, in *The Treasures of Eureka, I: Electron Paramagnetic Resonance: From Fundamental Research to Pioneering Applications & Zavoisky Award*, Ed. K. M. Salikhov, AXAS, Wellington, 2009, 122.
19. M. V. Fedin, S. L. Veber, R. Z. Sagdeev, V. I. Ovcharenko, E. G. Bagryanskaya, *Izv. Akad. Nauk, Ser. Khim.*, 2010, 1043 [*Russ. Chem. Bull., Int. Ed.*, 2010, **59**, 1065].
20. M. Fedin, V. Ovcharenko, R. Sagdeev, E. Reijerse, W. Lubitz, E. Bagryanskaya, *Angew. Chem., Int. Ed.*, 2009, **47**, 6897.
21. Yu. A. Osip´yan, R. B. Morgunov, A. A. Baskakov, V. I. Ovcharenko, S. V. Fokin, *Fiz. Tverd. Tela*, 2003, **45**, 1396 [*Phys. Solid State (Engl. Transl.)*, 2003, **45**, 1465].
22. E. M. Zueva, E. R. Ryabykh, A. M. Kuznetsov, *Izv. Akad. Nauk, Ser. Khim.*, 2009, 1605 [*Russ. Chem. Bull., Int. Ed.*, 2009, **58**, 1654].
23. A. V. Postnikov, A. V. Galakhov, S. Blügel, *Phase Transitions*, 2005, 689.
24. S. Vancoillie, L. Rulíšek, F. Neese, K. Pierloot, *J. Phys. Chem. A*, 2009, **113**, 6149.
25. V. A. Morozov, N. N. Lukzen, V. I. Ovcharenko, *J. Phys. Chem. B*, 2008, **112**, 1890.
26. V. A. Morozov, N. N. Lukzen, V. I. Ovcharenko, *Izv. Akad. Nauk, Ser. Khim.*, 2008, 849 [*Russ. Chem. Bull., Int. Ed.*, 2008, **57**, 863].
27. V. A. Morozov, N. N. Lukzen, V. I. Ovcharenko, *Dokl. Akad. Nauk*, 2010, **430**, 647 [*Dokl. Phys. Chem. (Engl. Transl.)*, 2010, **430**, 33].
28. V. I. Ovcharenko, in *Stable Radicals: Fundamentals and Applied Aspects of Odd-Electron Compounds*, Ed. R. Hicks, Wiley—VCH, New York, 2010, 461.

29. *Cambridge Structural Database, Version 5.31*, Cambridge Crystallographic Data Centre, Cambridge, November 2009 (last update August 2010).
30. F. Lanfranc de Panthou, D. Luneau, R. Musin, L. Öhrström, A. Grand, P. Turek, P. Rey, *Inorg. Chem.*, 1996, **35**, 3484.
31. R. N. Musin, P. V. Schastnev, S. A. Malinovskaya, *Inorg. Chem.*, 1992, **31**, 4118.
32. M. V. Fedin, S. L. Veber, G. V. Romanenko, V. I. Ovcharenko, R. Z. Sagdeev, G. Klihm, E. Reijerse, W. Lubitz, E. G. Bagryanskaya, *Phys. Chem. Chem. Phys.*, 2009, **11**, 6654.
33. E. V. Tret´yakov, S. V. Fokin, G. V. Romanenko, V. N. Ikorskii, A. V. Podoplelov, V. I. Ovcharenko, *Izv. Akad. Nauk, Ser. Khim.*, 2006, 64 [*Russ. Chem. Bull., Int. Ed.*, 2006, **55**, 66].
34. B. Bleaney, K. D. Bowers, *Proc. Roy. Soc. A*, 1952, **214**, 451.
35. S. L. Veber, M. V. Fedin, S. V. Fokin, R. Z. Sagdeev, V. I. Ovcharenko, E. G. Bagryanskaya, *Appl. Magn. Reson.*, 2010, **37**, 693.
36. M. V. Fedin, S. L. Veber, K. Yu. Maryunina, G. V. Romanenko, E. A. Suturina, N. P. Gritsan, R. Z. Sagdeev, V. I. Ovcharenko, E. G. Bagryanskaya, *J. Am. Chem. Soc.*, 2010, **132**, 13886.
37. Pat. WO 2005/019211 A2; *Chem. Abstr.*, 2005, **142**, 280195t.
38. G. T. Morgan, H. Burge, *J. Chem. Soc.*, 1921, **119**, 1546.
39. V. I. Ovcharenko, S. V. Fokin, P. Rey, *Mol. Cryst. Liq. Cryst.*, 1999, **334**, 109.
40. L. Carlin, *Magnetochemistry*, Springer-Verlag, Berlin, 1986.
41. F. B. Sviridenko, D. V. Stass, T. V. Kobzeva, E. V. Tretyakov, S. V. Klyatskaya, E. V. Mshvidobadze, S. F. Vasilevsky, Yu. N. Molin, *J. Am. Chem. Soc.*, 2004, **126**, 2807.
42. F. Neese, *ORCA — An Ab Initio, Density Functional and Semiempirical Program Package, Version 2.6, Revision 35*, University of Bonn, Bonn, 2008.
43. C. Adamo, M. Cossi, V. Barone, *J. Mol. Struct. (Theochem.)*, 1999, **493**, 145.
44. C. A. Daul, I. Ciofini, A. Bencini, in *Reviews of Modern Quantum Chemistry, Part II*, Ed. K. D. Sen, World Scientific, Singapore, 2002, 1247.
45. L. Noodleman, C. Y. Peng, D. A. Case, J. M. Mouesca, *Coord. Chem. Rev.*, 1995, **144**, 199.
46. L. Noodleman, J. G. Norman, Jr., *J. Chem. Phys.*, 1979, **70**, 4903.
47. E. R. Davidson, D. Feller, *Chem. Rev.*, 1986, **86**, 681.

Received February 18, 2011;
in revised form October 28, 2011